Correspondence to:
V. Marsili,
valentina.marsili@unife.it

Author Contributions:
Conceptualization: V. Marsili, S. Alvisi, S. Meniconi, B. Brunone, M. Franchini
Data curation: V. Marsili, S. Alvisi
Formal analysis: V. Marsili, S. Alvisi, F. Maietta, C. Capponi, S. Meniconi, B. Brunone, M. Franchini
Investigation: V. Marsili, S. Alvisi, F. Maietta, C. Capponi, S. Meniconi, B. Brunone, M. Franchini
Methodology: V. Marsili, S. Alvisi, M. Franchini
Project Administration: S. Alvisi, M. Franchini
Resources: V. Marsili, S. Alvisi, M. Franchini
Software: V. Marsili, S. Alvisi, C. Capponi
Supervision: V. Marsili, S. Alvisi, C. Capponi, S. Meniconi, B. Brunone, M. Franchini

Extending the Application of Connectivity Metrics for Characterizing the Dynamic Behavior of Water Distribution Networks

V. Marsili[1] , S. Alvisi[1] , F. Maietta[2] , C. Capponi[2] , S. Meniconi[2] , B. Brunone[2] , and M. Franchini[1]

[1]Department of Engineering, University of Ferrara, Ferrara, Italy, [2]Department of Civil and Environmental Engineering, University of Perugia, Perugia, Italy

Abstract Water distribution networks (WDNs) are complex combinations of nodes and links, and the current tendency is to modify their topological structure through the closure of isolation valves for monitoring and water quality reasons. For their analysis, several approaches based on graph theory have recently been proposed, mainly considering steady-state flow conditions. However, in their real functioning, WDNs are continuously subjected to pressure transients generated by maneuvers on regulation devices or by users' activity. This study investigates the application of some metrics from graph theory, already used in the context of steady-state analysis, for assessing the effects of changes in the topological structure of a network—due for example, to sectorization or branching operations—on its transient response when subjected to maneuvers on devices such as hydrants, pumps, etc. or users' activity. The analysis shows that some connectivity metrics can effectively reflect the dynamic pressure behavior of the network and, thus, provide useful indications for design and management operations taking into account unsteady flow features.

1. Introduction

Water distribution networks (WDNs) are designed and built with topological structures that are usually characterized by branches and loops. Branches ensure low design costs, whereas loops typically guarantee high hydraulic and mechanical reliability (Sirsant & Reddy, 2020; Todini, 2000). This implies the capability of dealing with particular hydraulic conditions due, for example, to very high water consumption or leakage and facing the outage of one or more pipes due, for example, to a burst or rehabilitation. In this regard, several methods have been proposed in the literature to identify an optimal topological structure that can ensure a balance between reliability and cost (e.g., Farmani et al., 2005; Mala-Jetmarova et al., 2018; Perelman et al., 2013; Prasad & Park, 2004). As a result, real WDNs are organized in very complex topological structures where, for example, the portions serving urban areas with a higher population density and water demand are typically characterized by a higher density of connections and greater redundancy of paths with pipelines of small length and diameter to ensure reliability and efficiency. On the contrary, sparser structures consisting of pipes of larger length and diameter are installed at the suburban level and for transmission mains.

Nowadays, WDNs topological structures are very often modified, and networks are frequently subjected to sectorization and branching operations by closing isolation valves (IVs). Indeed, along with the aspects related to network reliability, other issues of interest have emerged and are of concern to water utilities. This is the case, for example, of the observability and controllability of water networks and the compliance with certain operating conditions, for example, average and minimum water velocity in pipes to ensure sufficient water quality.

Concerning the observability aspects, looped systems are less controllable and, in recent years, a tendency toward reducing the interconnection of WDNs through, for example, sectorization techniques (i.e., District Metered Areas [DMAs] creation) has emerged. This practice consists in dividing a looped system into network portions (i.e., districts) that are connected at a limited number of sections, where flow meters are installed, whereas all the remaining interconnection sections are closed through IVs (e.g., Alvisi, 2015; Chondronasios et al., 2017). The closure of such IVs results in an alteration of the topological/connectivity structure of the WDN and a reduction in the number of loops. Procedures for identifying the optimal district layout are often based on optimization algorithms that require the resolution of a significant number of connectivity configurations (e.g., Hajebi et al., 2016; Zhang et al., 2017).

Validation: V. Marsili, S. Alvisi, F. Maietta, C. Capponi, S. Meniconi, B. Brunone, M. Franchini
Visualization: V. Marsili, S. Alvisi, F. Maietta, C. Capponi, S. Meniconi, B. Brunone, M. Franchini
Writing – original draft: V. Marsili, S. Alvisi, S. Meniconi, B. Brunone, M. Franchini
Writing – review & editing: V. Marsili, S. Alvisi, F. Maietta, C. Capponi, S. Meniconi, B. Brunone, M. Franchini

Concerning the compliance with certain operating conditions, strongly interconnected network structures result in a reduction of the average velocity in pipes. This feature implies (a) the aging of the water before it is delivered to users and the consequent reduction of the free residual chlorine or the formation of chlorination by-products (Quintiliani, 2017) and (b) the failure to reach the daily self-cleaning velocity (Abraham et al., 2017; Vreeburg & Boxall, 2007). Regarding this issue as well, several approaches have been developed to identify the optimal interventions on the topological structure of the network based, for example, on the closure of IVs and reduction of the level of interconnection to ensure optimal conditions in terms of velocity (Brentan et al., 2021; Marquez Calvo et al., 2018; Quintiliani et al., 2019). Again, the optimal set of IVs to be closed is often identified through optimization algorithms evaluating a very large number of solutions.

In the last decades, graph theory and connectivity-based methods have been proposed to solve problems related to sectorization and DMAs creation (e.g., Di Nardo & Di Natale, 2011; Giustolisi & Ridolfi, 2014a, 2014b; Huang et al., 2020; Tzatchkov et al., 2006; Yazdani & Jeffrey, 2012), and operating conditions and water quality aspects (Furnass et al., 2013; Grayman et al., 2009; Sitzenfrei, 2021). More generally, graph theory and connectivity-based methods are nowadays applied in a wide range of fields (Alderson, 2008; Strogatz, 2001) and have gained increasing attention also for pipe networks proving to be useful tools, especially if properly integrated with hydraulic theory (Torres et al., 2016).

However, in all the previously mentioned studies, graph theory and connectivity-based metrics are applied to support the optimal sectorization and IVs closure, mainly under the assumption of steady-state conditions. On the other hand, several studies have shown that, in their real functioning, WDNs rarely achieve steady-state conditions for more than a small fraction of their operational time and are subjected to continuous pressure variations. These can be due to maneuvers on the main devices in the network, such as turning on/off of pumps, fast opening/closing of hydrants for pipe flushing, or fire emergency. These maneuvers can result in significant pressure changes and consequent immediate damage, for example, pipe burst or collapse, vibrations, cavitation, and risk of contamination at cross-connections (Boulos et al., 2005). Recently, there has been evidence that users' activity (Marsili et al., 2021), that is, the opening and closing of domestic devices, can also result in the generation of pressure waves of small entity but occurring almost continuously over the day, producing deterioration that tends to worsen over time and increase failure rate (Rezaei et al., 2015).

Some studies have shown that the response of the WDN to these forcing factors depends on its characteristics and, in particular, on the topological structure (i.e., network connectivity) (Meniconi et al., 2022a, 2022b) as well as the presence of elements such as dead ends (Meniconi et al., 2018, 2021) and on diameter and material of pipes (Ellis, 2008; Karney & McInnis, 1990; Starczewska et al., 2014). Thus, each WDN is characterized by a different transient response in the face of a forcing factor. A variation in the system transient response can also be expected when its topological structure is modified by closing IVs to improve observability or operating conditions, as highlighted above. Nonetheless the impact that topology modifications can potentially have on the transient response of WDNs, an explicit focus on the role of pipe network topology on the unsteady flow behavior of WDNs has not been widely investigated.

From an operational standpoint, the dynamic behavior of a WDN with a given topological structure and subjected to a given forcing factor can be evaluated through unsteady flow numerical simulations. However, in the case of real, complex WDNs, this approach can be extremely expensive from a computational point of view, especially when simulations have to be carried out for a significant number of configurations. An open aspect, not properly addressed so far in the literature, is related to the use of graph theory—notoriously computationally unexpensive—for the analysis and/or management of water WDNs extending the application of connectivity metrics (CMs) from a steady-state framework to a dynamic one.

This study aims to evaluate the ability of five CMs derived from graph theory—already used for assessing network reliability under steady-state conditions—to provide useful insights into the effects of the topological structure changes due to the closure of selected IVs on the transient response of a WDN. The connectivity indicators considered in the study are introduced in the following section. The method adopted is then presented and applied to a simple lattice network and to a real WDN subjected to different transient scenarios. The obtained results are discussed and, finally, some conclusive considerations are offered.

2. Materials and Methods

In this section, transient modeling details are reported. The CMs considered in the analysis are then introduced and the method aimed at evaluating their ability to reflect useful information on the effects of the topological structure of a WDN on its transient response is presented. Subsequently, the two networks (i.e., a simple lattice network and a real network) to which the method is applied are introduced.

2.1. Transient Modeling

In this study, the approach used to simulate the dynamic behavior of a WDN is based on the continuity:

$$\frac{\partial h}{\partial t} + \frac{c^2}{g} \frac{\partial V}{\partial x} = 0 \tag{1}$$

and momentum equation:

$$\frac{\partial h}{\partial x} + \frac{V}{g} \frac{\partial V}{\partial x} + \frac{1}{g} \frac{\partial V}{\partial t} + J = 0 \tag{2}$$

where h = piezometric head, V = mean flow velocity, c = pressure wave speed, x = spatial co-ordinate along the pipe, t = temporal co-ordinate, g = gravitational acceleration, and J = friction term (Wylie & Streeter, 1993).

When fast transients are considered, according to the literature (e.g., Ghidaoui et al., 2005), the friction term, J, is assumed as a sum of the steady-state component, J_s, and the unsteady-state component, J_u:

$$J = J_s + J_u \tag{3}$$

The steady-state component is evaluated by the Darcy-Weisbach equation ($J_S = fV|V|/2g\phi$, with f = friction coefficient, V = local instantaneous value of the mean flow velocity, and ϕ = internal diameter).

The unsteady-state component accounts for the quite different behavior of the velocity gradient at the pipe wall with respect to the uniform-flow one with the same V (Brunone & Berni, 2010; Sundstrom & Cervantes, 2017). Studies demonstrate that the omission of such a term in the numerical model produces a smaller decay of the pressure with respect to the measured ones (e.g., Ebacher et al., 2011). As shown by Marsili et al. (2022), the choice of the unsteady friction model cannot disregard the characteristics of the investigated pipe system. In the case of a complex WDN with a significant number of users, the need is to make the numerical simulations affordable in terms of computational time, data storage, and memory. This automatically makes the choice fall on instantaneous acceleration-based models (Bergant et al., 2001; Brunone & Golia, 2008; Brunone et al., 1995). In this paper, the model proposed in Brunone et al. (1995) and modified by Pezzinga (2000) is adopted:

$$J_U = \frac{k_B}{g}\left(\frac{\partial V}{\partial t} + \text{sign}\left(V\frac{\partial V}{\partial x}\right)c\frac{\partial V}{\partial x}\right) \tag{4}$$

where the decay coefficient, k_B, is given by the relationship proposed by Vardy and Brown (1996):

$$k_B = \frac{\sqrt{C^*}}{2} \tag{5}$$

with $C^* = \min\{0.00476; 7.41/\text{Re}^\kappa\}$ where $\text{Re} = V\phi/\nu$ is the local instantaneous Reynolds number, and $\kappa = \log_{10}\left(14.3/\text{Re}^{0.05}\right)$.

Equations 1 and 2 are integrated by the Method of Characteristics (MOC) and transformed into the set of algebraic compatibility equations reported below:

$$C^+ : h_i^t = C_P - B_P Q_i^t \tag{6}$$

$$C^- : h_i^t = C_N + B_N Q_i^t \tag{7}$$

valid along the straight characteristic lines, C^+ and C^-, with subscript i and superscript t indicating the location and time, respectively (Wylie & Streeter, 1993). Within the MOC, the pipe is divided in reaches with a length

$\Delta s = c\Delta t$, being Δt the simulation time step. Coefficients C_P, C_N, B_P, and B_N are known quantities depending on the values of the discharge and piezometric head at the previous time steps:

$$C_P = h_{i-1}^{t-\Delta t} + BQ_{i-1}^{t-\Delta t} - \frac{k_B \Delta s}{g\Omega}\left(\frac{Q_{i-1}^{t-\Delta t} - Q_{i-1}^{t-2\Delta t}}{\Delta t} + \text{sign}\left(Q_i^{t-\Delta t}\right)\left|\frac{Q_i^{t-\Delta t} - Q_{i-1}^{t-\Delta t}}{\Delta s}\right|c \right) \tag{8}$$

$$C_N = h_{i+1}^{t-\Delta t} - BQ_{i+1}^{t-\Delta t} + \frac{k_B \Delta s}{g\Omega}\left(\frac{Q_{i+1}^{t-\Delta t} - Q_{i+1}^{t-2\Delta t}}{\Delta t} + \text{sign}\left(Q_i^{t-\Delta t}\right)\left|\frac{Q_i^{t-\Delta t} - Q_{i+1}^{t-\Delta t}}{\Delta s}\right|c \right) \tag{9}$$

$$B_P = B + R|Q_{i-1}^{t-\Delta t}|, \tag{10}$$

$$B_N = B + R|Q_{i+1}^{t-\Delta t}| \tag{11}$$

where B ($=c/(g\Omega)$) is the characteristic impedance, Ω = pipe cross-sectional area, and R ($=f\Delta s/(2g\phi\Omega^2)$) is the pipe resistance coefficient.

Pre-transient pressure at the nodes and initial discharge in the links are determined by solving the network using the Global Gradient Algorithm (Todini & Pilati, 1988).

Boundary conditions are the reservoir and the junction with an outflow discharge (Wylie & Streeter, 1993). The reservoir is assumed to model the inlet points of a network with a constant piezometric head. The junction with a nodal outflow, q_i^t, is implemented to simulate the discharge of a hydrant but also the user's connection; the corresponding piezometric head at the i-th junction at a given time, t, has been obtained by the following equation:

$$h_i^t = C_n - B_n q_i^t \tag{12}$$

where $C_n = \frac{\sum C_P/B_P + \sum C_N/B_N}{\sum 1/B_P + \sum 1/B_N}$, and $B_n = \frac{1}{\sum 1/B_P + \sum 1/B_N}$ include all the links connected to the junction (Wylie & Streeter, 1993). Then, Equations 6 and 7 yield the discharge in each link.

From the compatibility equations, that is, Equations 6 and 7, the reflection, r, and the transmission coefficient, s, can be derived (Misiunas, 2005; Swaffield & Boldy, 1993):

$$r = \frac{\frac{\Omega_j}{c_j} - \sum_{\substack{i=1 \\ i \neq j}}^{np} \frac{\Omega_i}{c_i}}{\sum_{i=1}^{np} \frac{\Omega_i}{c_i}} \tag{13}$$

$$s = \frac{\frac{2\Omega_j}{c_j}}{\sum_{i=1}^{np} \frac{\Omega_i}{c_i}} \tag{14}$$

where subscript i (ranging from 1 to np, np being the number of pipes merging at the node) indicates the pipes connected to the node and subscript j indicates the pipe from which the pressure wave arrives. These coefficients regulate the interaction mechanisms of reflection and transmission of an incoming pressure wave at each singularity. The topological structure of a WDN is the combination of all its singularities and the transient response of the network due to a forcing factor is the global result of the reflection and transmission of single pressure waves at each singularity.

For a constant level reservoir, the reflected pressure wave is equal in magnitude to that of the incident wave but with an opposite sign, or $r = -1$. For a dead end or a fully closed valve, the reflected pressure wave has the same magnitude and sign of the incident wave, or $r = +1$ (Chaudhry, 2014).

From an operational standpoint, the simulation model based on MOC has been implemented in MATLAB® (version 2019b).

2.2. Connectivity Metrics

To investigate the possible relationship between the CMs of WDNs and their dynamic behavior, five metrics—already proposed in the literature and used within the framework of graph theory—are considered. In greater detail, to represent the network properties two types of CMs are considered: the combinatoric-based graph theory metrics and the spectral metrics (Torres et al., 2016).

Combinatoric-based metrics mainly depend on the number of nodes n and links m of the network and indicate the degree of connectivity of vertices (i.e., nodes) and edges (i.e., links). Spectral metrics analyze the spectrum of network characteristic matrixes, such as the adjacency matrix, $[n \times n]$. For a network undirected graph, this matrix indicates which vertices are connected (i.e., adjacent). In fact, the generic element a_{ij} of the adjacency matrix **A** assumes a value equal to 1 if the nodes i and j are directly connected; otherwise, it is equal to 0. For real networks, adjacency matrix **A** is real and symmetrical and, therefore, its eigenvalues are real. Spectral metrics relate the topology of the network to its robustness, or its tolerance to faults, and are employed to quantify well-connectedness and the strength of the network connections (Torres et al., 2016; Yazdani & Jeffrey, 2010).

In this study, three combinatoric-based metrics and two spectral metrics are considered, for a total of $N_{\text{CM}} = 5$ CMs. The first combinatoric-based metric considered is the average degree, $\overline{d}$:

$$\overline{d} = \frac{1}{n} \sum_{i=1}^{n} d_i \tag{15}$$

where the nodal degree d_i of node i is the number of links converging at node i. The average degree, $\overline{d}$, can be also evaluated by using the number of nodes n and links m of the network:

$$\overline{d} = \frac{2m}{n} \tag{16}$$

This metric assumes values in the range $\left[2 - \frac{2}{n}; n - 1\right]$, where the extreme values are evaluated considering the minimum and maximum number of links in a connected graph: $m_{\min} = n - 1$ and $m_{\max} = \frac{n(n-1)}{2}$. Average degree indicates the overall sparseness of the network configuration, where a sparse network is defined as a network with the number of links linearly proportional to the number of nodes (Diestel, 2005). Sparseness is opposed to density, the latter describing the relationships on the quantity of existing pipes versus the maximum number of possible pipe connections (Torres et al., 2016).

The second combinatoric-based metric considered is the meshedness coefficient, R_m, defined by the ratio between the total number $o = m - n + 1$ of independent loops and the maximum theoretical number $o_{\max} = 2n - 5$ of independent loops in the network:

$$R_m = \frac{m - n + 1}{2n - 5} \tag{17}$$

This metric ranges between 0, when the number o of independent loops in the network is equal to 0, and 1, when the number o of independent loops in the network is maximum (i.e., equal to $o_{\max}$). The meshedness coefficient, growing with the number of loops, can effectively describe the redundancy of the network. It indicates the presence of independent alternative paths between the source and demand nodes which can be used to satisfy supply requirements during the disruption or failure of the main paths (Yazdani & Jeffrey, 2010, 2012).

The third and last combinatoric-based metric selected is the number of single-degree nodes, DE, that corresponds to the total number of nodes in a network with a node degree d equal to 1:

$$\text{DE} = \sum_{i=1}^{n} sd_i; \text{ where } sd_i = \begin{cases} 1 & \text{if } d_i = 1 \\ 0 & \text{otherwise} \end{cases} \tag{18}$$

Accordingly, DE is equal to the number of dead ends within a pipe network (Newman, 2010; Torres et al., 2016) assuming values in the range $[0; m]$.

Concerning spectral metrics, the spectral gap, $\Delta\lambda$, and the algebraic connectivity, λ_2, are considered.
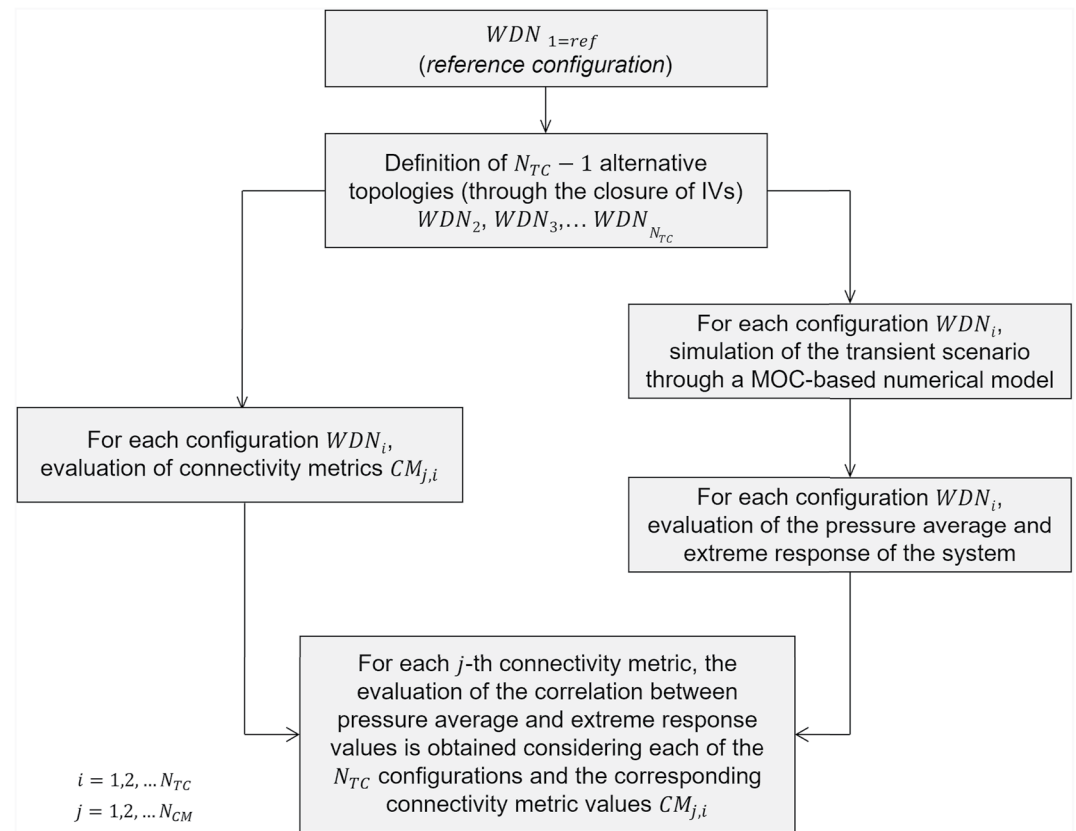
Figure 1. Proposed methodology.

The spectral gap $\Delta\lambda$ is defined as the difference between the first and second eigenvalues of the adjacency matrix **A** of the network and it is effective in quantifying the Good Expansion properties of the system. In particular, networks characterized by high value of $\Delta\lambda$ present a topological structure with a limited presence of bottlenecks, articulation points, or bridges whose removal may split the network into two or more isolated parts and whose vertices are connected robustly to other nodes, even if the graph is not dense with links (Estrada, 2006). For WDNs, the spectral gap generally ranges between 0 and 1.5 (Giudicianni et al., 2018).

The algebraic connectivity, λ_2, corresponds to the second smallest eigenvalue of the Laplacian matrix, $\mathbf{L} = \mathbf{D} - \mathbf{A}$, of the network (Fiedler, 1973), where **D** is the diagonal matrix of nodal degrees d_i. While the smallest eigenvalue of graph Laplacian is zero and its multiplicity equals the number of connected components in a network, a larger value of the algebraic connectivity λ_2 indicates the fault tolerance of the network and its robustness against efforts to cut it into parts (Yazdani & Jeffrey, 2010). λ_2 is non-zero if and only if a network is connected, that is it consists of a single component, and it ranges between 0 and 2 (Newman, 2010).

2.3. Methodology

To evaluate the applicability of the previously introduced metrics for the characterization of changes in the transient response of a WDN when its topological structure is modified, the approach described below, whose scheme is reported in Figure 1, is adopted.

Let us consider a generic WDN of given topological characteristics and assume that the WDN includes n nodes and m links for a total of o loops ($o = m - n + 1$). Let its original topological characteristics be hereinafter referred to as *reference configuration*, WDN$_{1=ref}$. Starting from the *reference configuration*, additional topological configurations WDN$_i$ (with $i = 2 : N_{TC}$, being N_{TC} the total number of considered topological configurations) can be defined by closing IVs and thus removing the corresponding links (e.g., to create districts or to improve water quality aspects).

On the one hand, for each network topological configuration WDN_i (with $i = 1 : N_{\text{TC}}$) the connectivity metrics values $\text{CM}_{j,i}$ (with $j = 1, 2, \ldots, N_{\text{CM}}$) can be computed. In the current study, the previously introduced metrics ($N_{\text{CM}} = 5$) are considered.

On the other hand, in the event of generic forcing factors acting in the network—such as the closing/opening of a valve or the switch on/off of a pump—pressure waves will be generated and propagate throughout the network according to its topological configuration, WDN_i. The interaction of pressure waves with WDN topological structure will generate time-varying pressure changes at each node.

On a defined time window, the effects in terms of pressure surge can be evaluated by means of the MOC-based model. In particular, for each node, the value of $\Delta p = p_{\max} - p_{\min}$ can be computed. It represents the range in which the pressure fluctuates at the node during the whole simulation, $p_{\max}$ and $p_{\min}$ being the maximum and minimum values of the simulated pressure signal p at the node during the considered time window.

In terms of the Δp-values observed at each node of the network, the effects on the whole system can be summarized for a given network topological configuration WDN_i through the cumulative frequency distribution (CFD_i) of the Δp values at all nodes. Furthermore, the values at the 50th and 90th percentiles of the CFD_i—henceforth indicated as $\Delta p_{50,i}$ and $\Delta p_{90,i}$—can be considered as representative of the average and extreme transient response of such a configuration, respectively. For the *reference configuration* (i.e., $i = 1$), the average and extreme transient response are hereinafter indicated as $\Delta p_{50,\text{ref}}$ and $\Delta p_{90,\text{ref}}$, respectively.

In order to compare the presumably different response of the network topological configuration WDN_i with respect to the *reference* one, the ratios $\frac{\Delta p_{50,i}}{\Delta p_{50,\text{ref}}}$ and $\frac{\Delta p_{90,i}}{\Delta p_{90,\text{ref}}}$ are evaluated for all the N_{TC} topologies.

Finally, the ability of each connectivity metric CM_j (with $j = 1, 2, \ldots, N_{\text{CM}}$) to provide useful insights into the effects of topological structure changes on the average and extreme transient responses of the network is evaluated considering the correlation between $\text{CM}_{j,i}$ and the corresponding pressure variation indicators $\frac{\Delta p_{50,i}}{\Delta p_{50,\text{ref}}}$ and $\frac{\Delta p_{90,i}}{\Delta p_{90,\text{ref}}}$ (with $i = 1 : N_{\text{TC}}$).

2.4. Case Studies

The above proposed method is applied to two WDNs, a simple lattice and a real one. The description of the two networks and details on the application of the transient model to each WDN are reported in the following.

2.4.1. The Simple Lattice Network

A simple WDN is first considered, whose scheme is reported in Figure 2a. The network presents a lattice layout featuring $o = 16$ loops. At the end of each pipe an IV is placed, that can be closed to create different network layouts. Overall, 80 IVs are installed. From an operational standpoint, each IV is modeled as a short link delimited by two nodes and its closure implies the removal of the link associated with it. In Figure 2, only numbers of main nodes (i.e., the ones representing vertices of the loops) are reported whereas black valves represent closed IVs (i.e., removed links).

The network is supplied by a reservoir located at node 1, where a constant head of 35 m is imposed, and all pipes are characterized by the same diameter, ϕ (DN125), length, l (100 m), and wave speed, c (500 m/s). This looped layout will henceforth be referred to as the original or *reference configuration* or $\text{WDN}_{1=\text{ref}}$. Starting from the *reference configuration*, additional configurations, characterized by an equal number of nodes, n, but different number of links, m, were created by removing a growing number of short links corresponding to closed IVs leading to a total number of configurations $N_{\text{TC}} = 52$, including the *reference* one. For each configuration the links corresponding to closed IVs to be removed were randomly selected ensuring in any case that all nodes were connected to the reservoir. As an example, three of this $N_{\text{TC}} - 1$ additional configurations, obtained by closing an increasing number of IVs (12, 15, and 16) and indicated as WDN_2, WDN_3, and WDN_4, are also reported in Figures 2b–2d.

The transient scenario to which the lattice network was subjected consists in a maneuver generating a pressure wave at a node, representing for example, a hydrant. In greater detail, the maneuver consists in an almost instantaneous reduction from 5 to 0.05 L/s of the discharge at a given node, while no maneuvers are executed at the other nodes. To evaluate the global response of each configuration of the lattice network, more than one scenario per
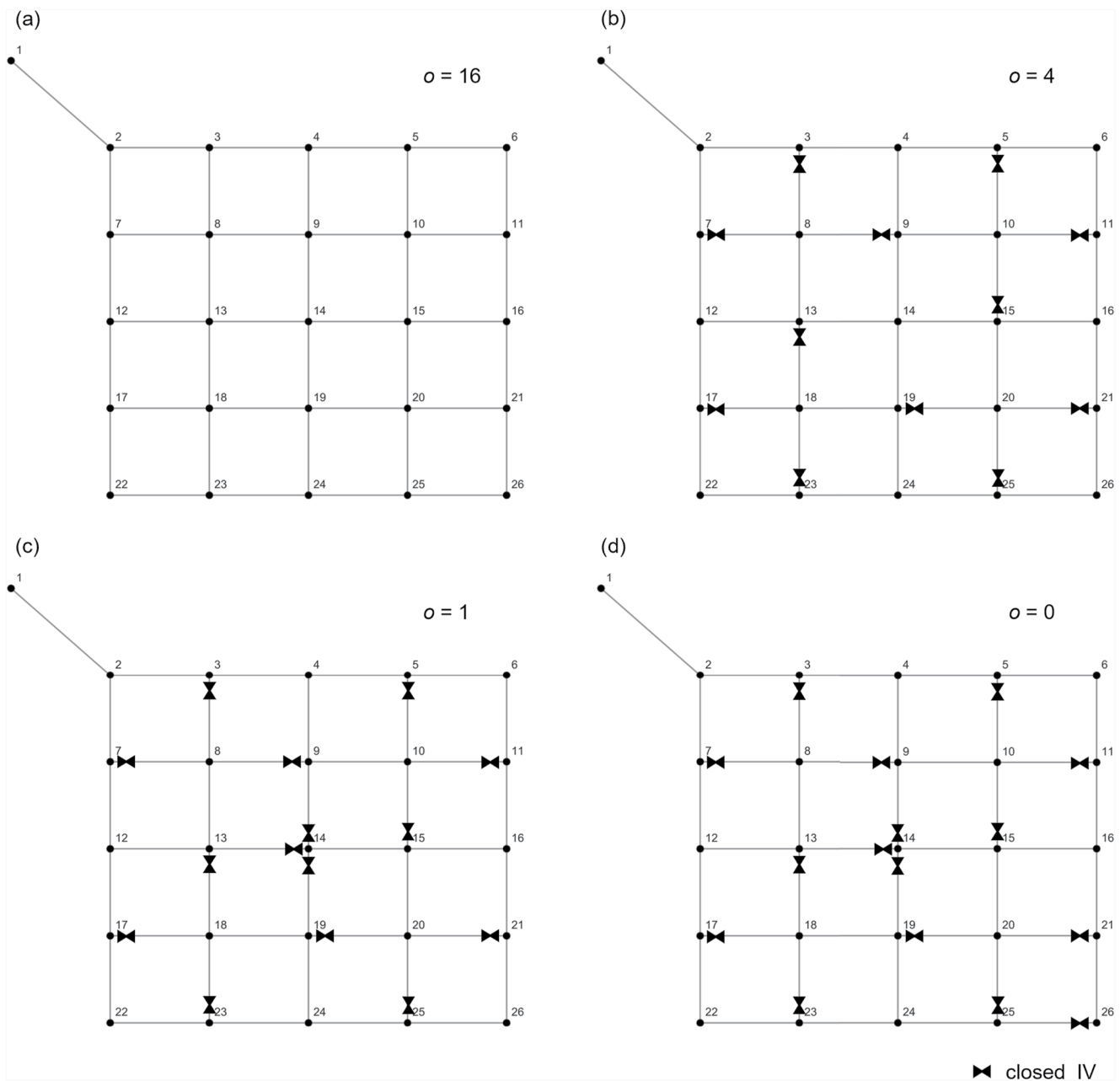
Figure 2. Layout of the simple network in configuration (a) $WDN_{1=ref}$, (b) WDN_2, (c) WDN_3, and (d) WDN_4. Note that only numbers of main nodes are reported whereas black valves represent closed isolation valves corresponding, by a computational point of view, to removed short links.

configuration was evaluated. In fact, for each one of the N_{TC} configurations, the fast reduction of the discharge at one node (from 3 to 26) at a time was considered and, consequently, 24 scenarios were produced and as many corresponding hydraulic simulations were conducted. The WDN transient response was evaluated considering a simulation time window, t_{sim}, equal to 30 s. This simulation time was chosen so as to gather the development of the pressure wave generated in the generic node, having in mind the characteristics of the network (i.e., pipe lengths and pressure wave speeds). The time step of the simulation Δt was assumed equal to 0.002 s and a slight adjustment of lengths was applied to respect the Courant condition (Wylie & Streeter, 1993).

2.4.2. The Real WDN

The second case study considered is a real complex WDN (Alvisi & Franchini, 2006), the layout of which is shown in Figure 3. The system, which has an almost constant altimetry, has a total length of approximately 90 km

Figure 3. Layout of the real water distribution network.

of cast-iron and steel pipes with diameter ranging from 25 to 600 mm and it is supplied by a reservoir. 50.000 inhabitants are supplied by the WDN corresponding to an average total net inflow of about 165 L/s.

The network consists of $n = 1,507$ nodes and $m = 1,795$ pipes, of which 844 are IVs, for a total of $o = 289$ loops. In the numerical simulations, a constant head of 30 m was imposed at the reservoir (i.e., node 1) and a constant value of the pressure wave speed, c, was assumed for cast-iron ($c = 900$ m/s) and steel ($c = 1,000$ m/s) pipes (Pothof & Karney, 2012). With reference to the pressure wave speed, constant values were assumed irrespectively of the diameter and the wall thickness. In fact, a sensitivity analysis confirms that slight variations of this parameter, due to the different value of the pipe diameter and thickness, do not impact significantly on the numerical results. Starting from the original configuration, that is, the *reference configuration* of the network where all the IVs are open, different configurations were obtained with an increasing number of branches. The progressive closure of the IVs in the network gave a total of $N_{TC} = 126$ configurations, including the *reference configuration*. In the creation of the different configurations, the full connectivity of the system and decreasing pipe diameters toward the downstream areas of the network were guaranteed.

For the real WDN, a different type of transient scenario with respect to the lattice network was considered. The WDN was assumed to be subjected to users' activity, that is, the closing/opening of domestic devices, that can stress the network with small entity pressure waves, almost continuous in time but also distributed in space, as highlighted in recent studies (e.g., Marsili et al., 2021). The approach for the characterization of water consumption proposed in Marsili et al. (2022) was adopted. In fact, use was made of demand time series at the level of individual users, with a 1-s time step, but observed in another network. These series were aggregated at the nodal level so as to obtain for each node an average water demand equivalent to the average annual demand at that node, the latter statistic being available from consumption billing. Moreover, the variations in demand were simulated assuming a realistic maneuver time of a fraction of a second, that is, $t_{man} = 0.5$ s. Such a value has been suggested by the preliminary tests carried out at the Water Engineering Laboratory of the University of Ferrara aimed to derive the tap maneuvering time. The water demand scenario obtained was imposed for each one of the N_{TC} configurations.

For all the N_{TC} configurations, the simulation in unsteady flow conditions of the network subject to the user activity scenario was performed using the WDN transient model introduced above. A simulation time window $t_{sim} = 600$ s was applied to gather the development of pressure waves generated by users' and thus the dynamic behavior of the whole system. A time step of the simulation Δt equal to 0.01 s was assumed and each pipe was divided in an integer number of reaches by means of a slight adjustment of lengths in respect of the Courant condition.

3. Analysis of the Results

In the following, the results of the application of the proposed approach to the two WDNs are presented and the relationship between the $N_{CM} = 5$ CMs and their dynamic behavior is analyzed.

3.1. The Simple Lattice Network

First, the results of the application of the proposed approach to the simple lattice network and the $N_{TC} = 52$ defined configurations are analyzed. On the one hand, the N_{CM} CMs considered in the study was evaluated for each network topological configuration WDN$_i$ (with $i = 1 : N_{TC}$). On the other hand, for each network topological configuration WDN$_i$ unsteady flow simulations were executed in the face of 24 transient scenario of single maneuvers defined above. Based on the results obtained, some observations can be made.

As an example, in Figure 4 Δp is shown for each node of the network in configuration WDN$_{1=ref}$ (Figure 4a), WDN$_2$ (Figure 4b), WDN$_3$ (Figure 4c), and WDN$_4$ (Figure 4d) through a chromatic scale in the event of the fast
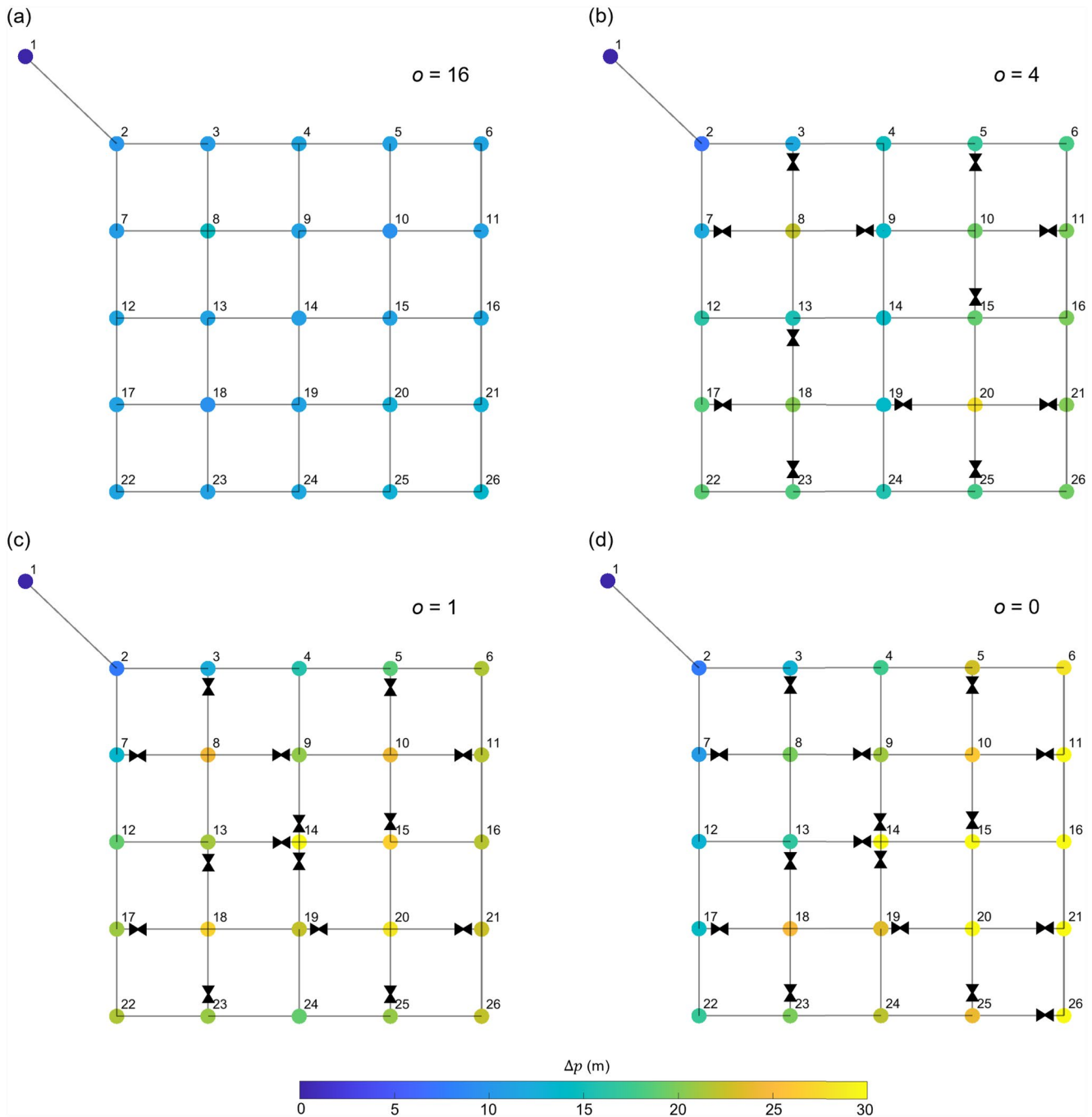
Figure 4. Δp variations at each node due to a fast closure at node 20 of the network in configuration (a) WDN$_{1=ref}$, (b) WDN$_2$, (c) WDN$_3$, and (d) WDN$_4$ obtained by unsteady flow simulation.

reduction (from 5 to 0.05 L/s) of the discharge at node 20. First, it is evident that the transient responses of the lattice network in the modified configurations (WDN$_2$, WDN$_3$, and WDN$_4$) are different from the response of the network in configuration WDN$_{1=ref}$, being the geometric characteristics, pipe diameters, wave speed and forcing factor the same for all the configurations. In particular, as the number of branches (interconnections) increases (decreases), a larger number of nodes are affected by a more significant Δp.

Similar results are obtained when other transient scenarios are considered, that is, when the fast closure is executed at a different node. Overall, the global response of the network in configuration WDN$_{1=ref}$, WDN$_2$, WDN$_3$, and
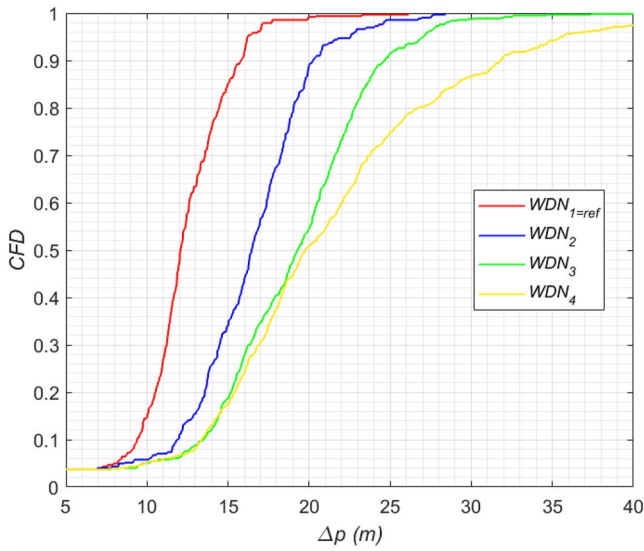
Figure 5. Cumulative frequency distributions of pressure variations Δp stressing the network nodes in different configurations.

WDN$_4$ due to all the single closure maneuvers carried out one at a time at each network node is described by the CFD of Δp at all main nodes (i.e., from 1 to 26) shown in Figure 5. The reciprocal position of the curves—and therefore the values of Δp_{50} and Δp_{90}—highlights that the topological structure influences the transient response of the system. In particular, as the number of branches in the network increases, the CFD of Δp tends to shift to the right.

Δp_{50} and Δp_{90} were evaluated by the CFD obtained for each one of the N_{TC} configurations. These parameters were considered representative of the average and extreme transient response of the given network configuration. In order to compare the response of a given network topological configuration WDN$_i$ (with $i = 1 : N_{TC}$) with respect to the *reference* one, the dimensionless response of the system at the 50th and 90th percentiles, $\frac{\Delta p_{50,i}}{\Delta p_{50,ref}}$ and $\frac{\Delta p_{90,i}}{\Delta p_{90,ref}}$, were determined.

In Figure 6, the dimensionless responses of the systems $\frac{\Delta p_{50,i}}{\Delta p_{50,ref}}$ and $\frac{\Delta p_{90,i}}{\Delta p_{90,ref}}$ considering all the $N_{TC} = 52$ configurations are related to the values of the $N_{CM} = 5$ CMs. Accordingly, each plotted point represents the relationship between the computed dynamic behavior of a WDN in a given configuration and the topological properties of such network configuration expressed in terms of a given CM. The stars refer to the lattice network in its *reference configuration* (or WDN$_{1=ref}$), whose response in terms of $\frac{\Delta p_{50,i}}{\Delta p_{50,ref}}$ and $\frac{\Delta p_{90,i}}{\Delta p_{90,ref}}$ is equal to one.

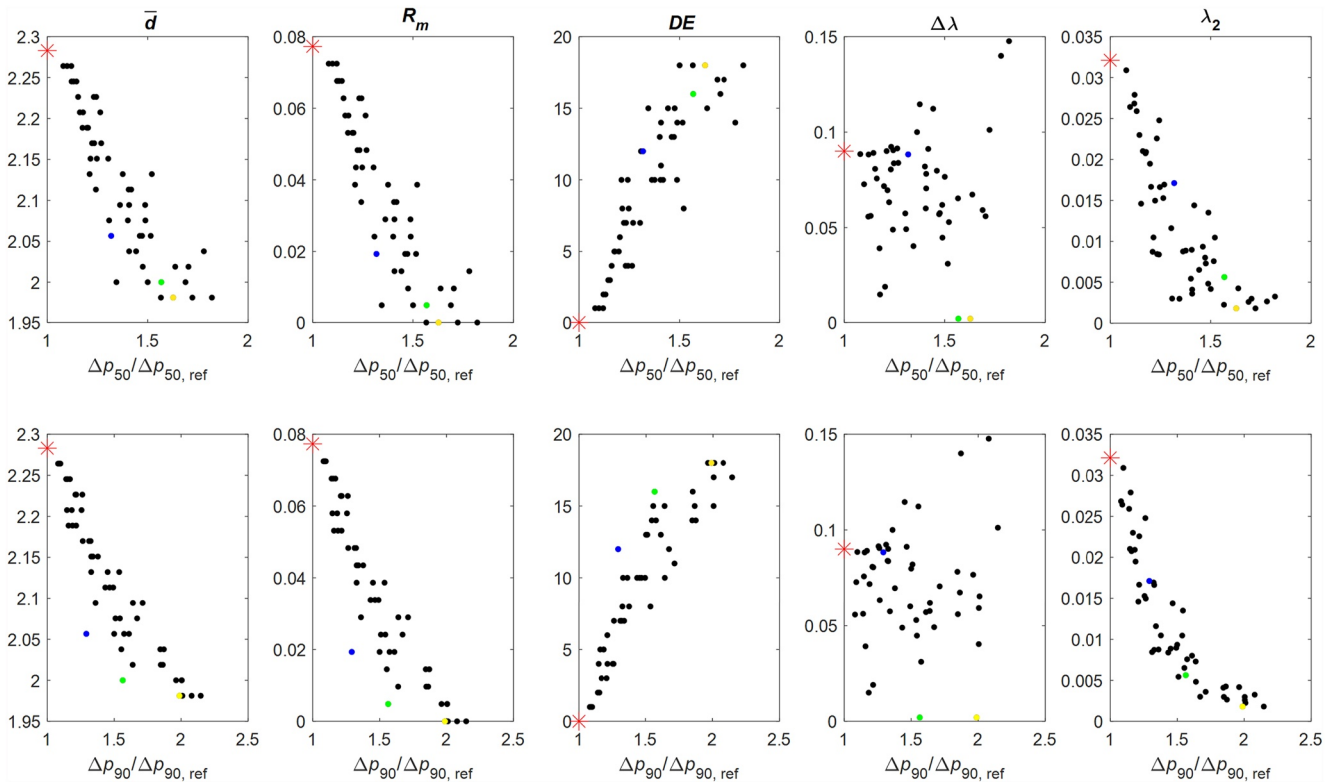**Figure 6.** Connectivity metrics ($\bar{d}$, R_m, DE, $\Delta\lambda$, and λ_2) as a function of the dimensionless transient responses of the water distribution network considered in the N_{TC} configurations. The stars indicate the network in its *reference configuration* whereas the blue, green, and yellow squares refer to configurations WDN$_2$, WDN$_3$, and WDN$_4$, respectively.

Table 1
Correlation Coefficient Matrix Assessed With Reference to the Transient Response of the Simple Lattice Network and the Values of the Connectivity Metrics, Evaluated by Means of Spearman's Rank Definition, ρ_S and Pearson Definition, ρ_P (Given in Brackets)

$\rho_S\,(\rho_P)$	$\Delta p_{50}/\Delta p_{50,\text{ref}}$	$\Delta p_{90}/\Delta p_{90,\text{ref}}$	$\overline{d}$	R_m	DE	$\Delta\lambda$	λ_2
$\Delta p_{50}/\Delta p_{50,\text{ref}}$	1.00 (1.00)	0.92 (0.89)	−0.91 (−0.89)	−0.91 (−0.89)	0.91 (0.89)	−0.05 (0.07)	−0.84 (−0.82)
$\Delta p_{90}/\Delta p_{90,\text{ref}}$		1.00 (1.00)	−0.95 (−0.92)	−0.95 (−0.92)	0.94 (0.92)	−0.09 (0.01)	−0.95 (−0.87)
$\overline{d}$			1.00 (1.00)	1.00 (1.00)	−0.99 (−0.99)	0.12 (0.06)	0.91 (0.90)
R_m				1.00 (1.00)	−0.99 (−0.99)	0.12 (0.06)	0.91 (0.90)
DE					1.00 (1.00)	−0.12 (−0.06)	−0.91 (−0.90)
$\Delta\lambda$						1.00 (1.00)	0.10 (0.04)
λ_2							1.00 (1.00)

First, it can be seen that as the number of branches in the network increases, and the number of loops decreases, $\overline{d}$, R_m, $\Delta\lambda$, and λ_2 tend to decrease while DE tends to increase. Moreover, it can be observed that there is a correlation between the average degree $\overline{d}$, meshedness coefficient, R_m, algebraic connectivity, λ_2, and number of single-degree nodes, DE, and the dynamic behavior of the system. Indeed, it can be observed from the quite regular point distributions that as the number of branches increases, and therefore as the redundancy of the network decreases, the transient response of the network is emphasized up to about 1.5 times compared to the average response $\Delta p_{50,\text{ref}}$ of the *reference configuration* (i.e., WDN$_{1=\text{ref}}$) and about 2 times compared to the extreme response $\Delta p_{90,\text{ref}}$. On the other hand, the spectral gap $\Delta\lambda$ is not effective in representing the dynamic behavior of the network as its configuration changes and responds with a scattered distribution.

These evaluations are quantitatively verified by determining the Spearman's rank correlation coefficient, ρ_S, and the Pearson correlation coefficient, ρ_P, between the CMs and the dimensionless average and extreme transient responses of the network, $\frac{\Delta p_{50}}{\Delta p_{50,\text{ref}}}$ and $\frac{\Delta p_{90}}{\Delta p_{90,\text{ref}}}$ (Table 1). The correlation analysis confirms that for $\overline{d}$, R_m, and λ_2 a strong negative correlation to the network response exists. Similarly, DE shows a strong positive correlation to the network response. On the contrary, $\Delta\lambda$ is only weakly correlated to the network response.

Some additional comments can be provided for the single CMs. Focusing the attention on the first two metrics, $\overline{d}$ and R_m, they provide the highest correlation coefficients with ρ_S values of about −0.91 and −0.95—and ρ_P values of −0.89 and −0.92, respectively—for the average and extreme response, respectively. Furthermore, they result perfectly correlated to each other given their direct relation with the number of nodes n and links m. Therefore, the benefit arising from their use is equivalent. At the same time $\overline{d}$ and R_m show a similar drawback. Indeed, they do not allow distinguishing configurations characterized by the same number of nodes, n, and links, m, but a different connectivity structure. In this study, the variations of $\overline{d}$ and R_m values are attributed to the change in the number of links, m, due to removing of links corresponding to closed IVs, given that the number of nodes, n, is the same for different configurations. As a result, different configurations featuring the same number of links m are characterized by the same value of the metrics $\overline{d}$ and R_m. Such a feature can be observed in Figure 6, where the points tend to be distributed along the horizontal line and each set of points in each line corresponds to different configurations with the same number of nodes and links. In practice, $\overline{d}$ and R_m cannot take into account the position of the valves that have been closed.

An increase of the number of closed IVs (i.e., a decrease in the number of links, m), the number of nodes n being equal, tends to increase the value of the metric DE, that is the number of dead ends in the network. In fact, the closure of an IV can generate at least one (see Figure 7a) but also a higher number of dead ends (see Figure 7b). In fact, the two configurations shown in Figures 7a and 7b present the same number of closed IVs (=2), and thus the same number of removed links and, accordingly, the same $\overline{d}$ and R_m values, but a different number of the generated dead ends (2 vs. 3). This aspect is the main reason behind the high but not perfect correlation between the first two metrics $\overline{d}$ and R_m and the third one, DE which, anyway, provides very high correlation coefficients with the network response, equivalent to $\overline{d}$ and R_m.

In addition, dead ends have an important role. In fact, pressure wave doubles at a dead end. Accordingly, many dead ends globally emphasizes the network response. Moreover, it is important to note that the increase of the number
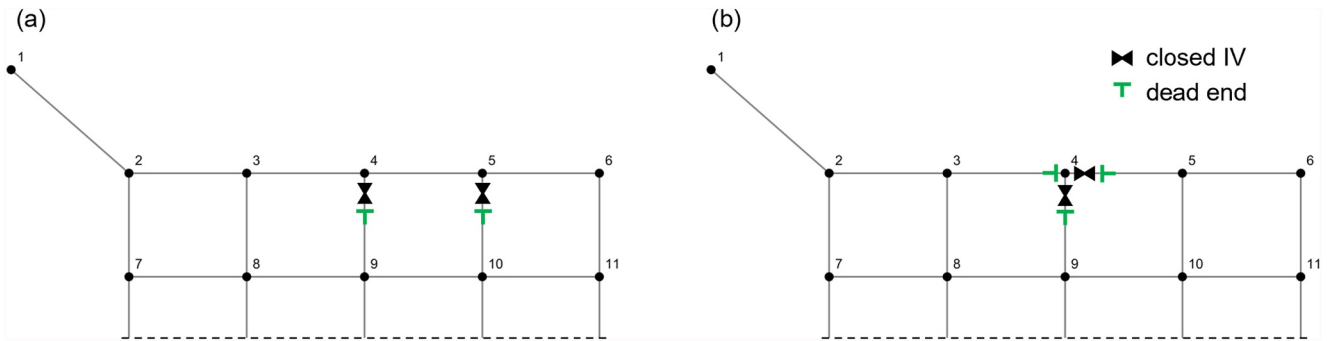
Figure 7. Example of two different network layouts featuring the same number of isolation valves (IVs) with a different number of dead ends: (a) closure of two IVs generating two dead ends and (b) closure of two IVs generating three dead ends.

of dead ends causes a decrease in the number of loops o in the system, the latter reflecting on the decrease of the meshedness coefficient R_m and its redundancy.

Considering the spectral metrics, they provide quite different performances. In fact, the spectral gap, $\Delta\lambda$, is not able to provide useful information, being the correlation coefficient very low. Indeed, drawbacks of this metric whenever applied for the characterization of WDN have been already pointed out by Torres et al. (2016) for steady-state conditions.

Concerning the last spectral metric, that is, the algebraic connectivity, λ_2, the obtained results can be interpreted recalling that the algebraic connectivity tends to decrease when network robustness decreases (Yazdani & Jeffrey, 2010). As highlighted above, a WDN is robust if great effort is needed to cut it into parts and this concept can be effectively caught by looking at the example shown in Figure 8. The network configuration in Figure 8a is less robust than the one in Figure 8b since the network on the left can be split in two parts by closing only one further IV (the one below node 9) whereas a greater number of closures is needed to disconnect the network configuration on the right. Indeed, values of the algebraic connectivity, λ_2, reflect this feature of these networks resulting 0.0080 for the network configuration on the left (Figure 8a) and 0.0095 for the network configuration on the right (Figure 8b).
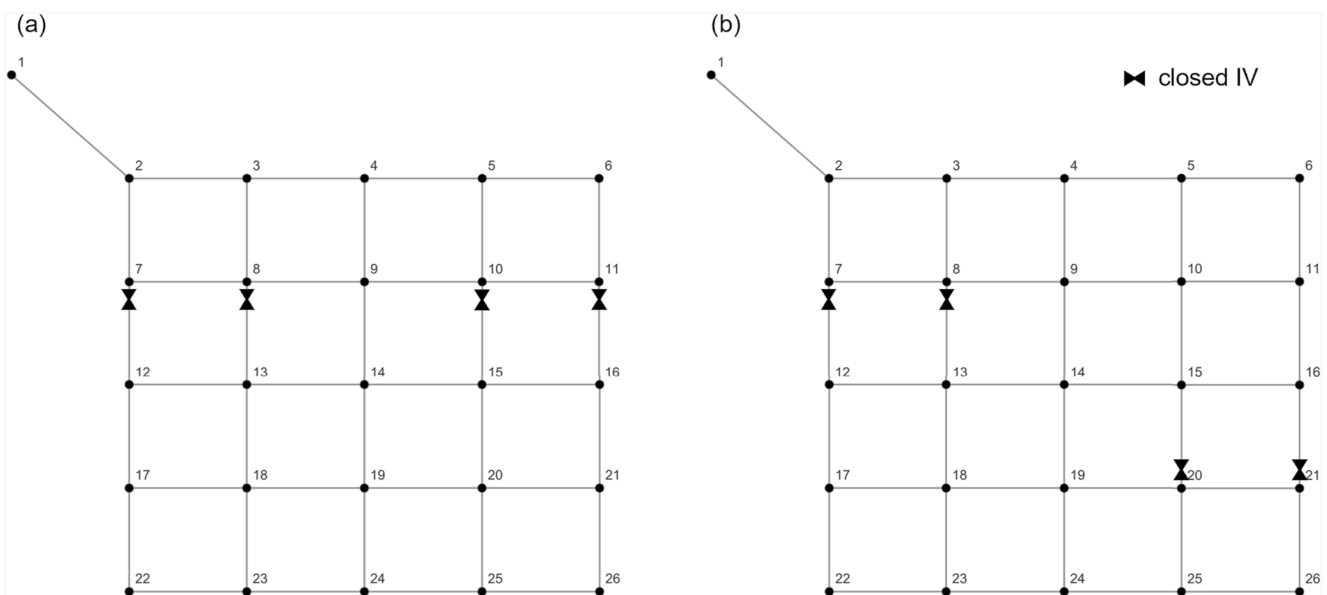

Figure 8. Example of two different network layouts featuring the same number of isolation valves but different algebraic connectivity λ_2: (a) $\lambda_2 = 0.0080$ and (b) $\lambda_2 = 0.0095$.
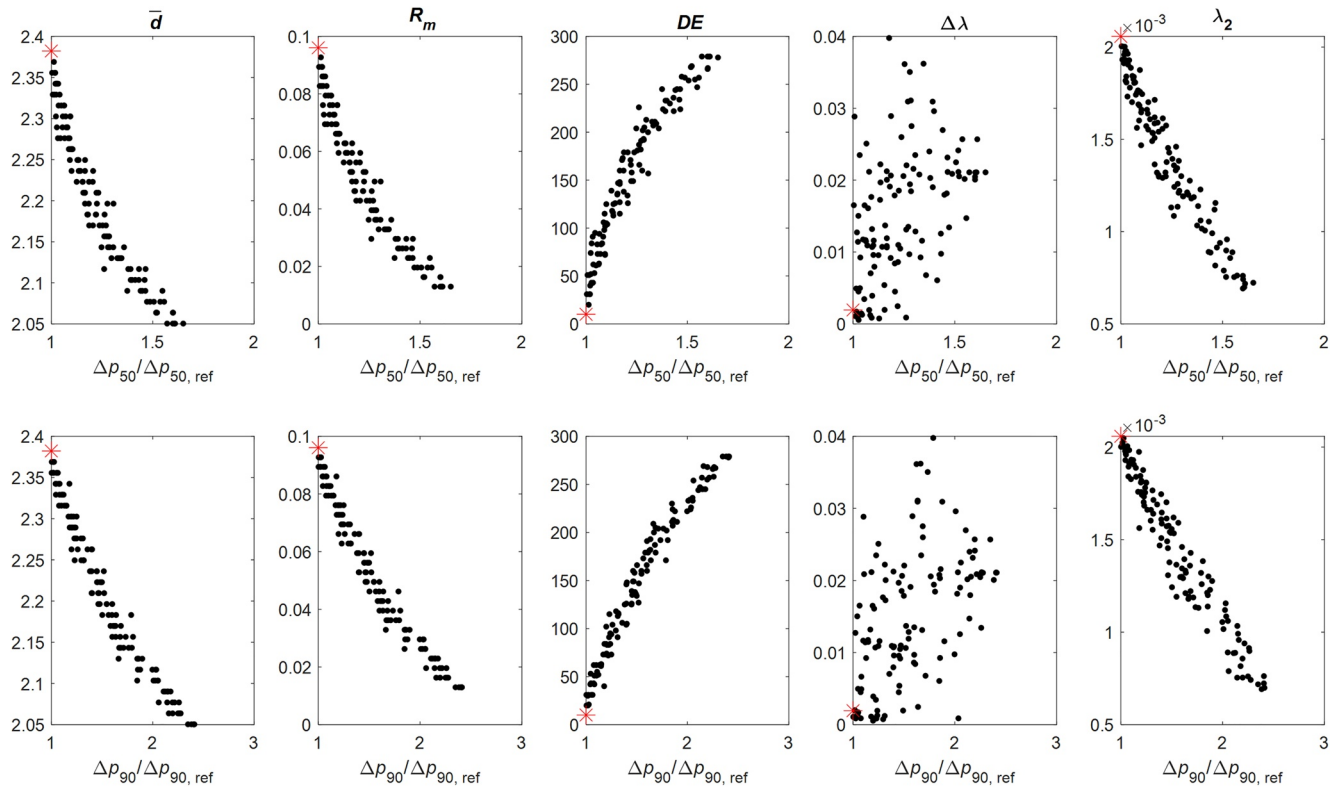
Figure 9. Connectivity metrics ($\overline{d}$, R_m, DE, $\Delta\lambda$, and λ_2) as a function of the dimensionless transient responses of the real network considered in the N_{TC} configurations. The stars indicate the network in its *reference configuration*.

All in all, it can be noted that the values of algebraic connectivity change in line with the meshedness coefficient, R_m (or the average node-degree $\overline{d}$) and this may be interpreted by stating that structural robustness in a network is positively correlated with the existence of loops redundancy (Yazdani & Jeffrey, 2012). However, if metrics performance is considered, the algebraic connectivity, λ_2, and the robustness concept embodied in its definition, shows slightly lower values of the correlation coefficient with respect to the meshedness coefficient, R_m, i.e., more directly related to the number of loops in the network.

3.2. The Real WDN

For each one of the $N_{TC} = 126$ configurations of the real WDN, the relationship between the values of the $N_{CM} = 5$ CMs and the dimensionless responses of the system, $\frac{\Delta p_{50}}{\Delta p_{50,ref}}$ and $\frac{\Delta p_{90}}{\Delta p_{90,ref}}$, evaluated by unsteady flow simulations in the face of the users' activity transient scenario, are shown in Figure 9. For each metric, the response of the *reference configuration* in terms of $\frac{\Delta p_{50}}{\Delta p_{50,ref}}$ and $\frac{\Delta p_{90}}{\Delta p_{90,ref}}$ is equal to one and is indicated by a star.

Also in the case of the real WDN, it can be observed that $\overline{d}$, R_m, DE, and λ_2 are effectively related to the dynamic behavior of the system, showing quite regular point distributions. On the other hand, the spectral gap, $\Delta\lambda$, is not effective in representing the dynamic behavior of the network as its configuration changes and responds once again with a scattered distribution.

This is confirmed by the Spearman's rank correlation coefficient, ρ_S, and the Pearson correlation coefficient, ρ_P, between the CMs and the dimensionless average and extreme transient responses of the network, $\frac{\Delta p_{50}}{\Delta p_{50,ref}}$ and $\frac{\Delta p_{90}}{\Delta p_{90,ref}}$, shown in Table 2. In fact, for $\overline{d}$, R_m, and λ_2 a strong negative correlation to the network response results. Similarly, DE shows a strong positive correlation to the network response. $\Delta\lambda$ is only weakly correlated to the network response also in the case of the real WDN.

Nonetheless the limits highlighted in the previous subsection, the metrics $\overline{d}$ and R_m provide again the highest correlation coefficients, with ρ_S values of about -0.98 and -0.99 and ρ_P values of -0.96 and -0.98, followed by DE and λ_2.

Table 2
Correlation Coefficient Matrix Assessed With Reference to the Transient Response of the Real Water Distribution Network and the Values of the Connectivity Metrics and Evaluated by Means of Spearman's Rank Definition, ρ_S and Pearson Definition, ρ_P (Given in Brackets)

$\rho_S\ (\rho_P)$	$\Delta p_{50}/\Delta p_{50,ref}$	$\Delta p_{90}/\Delta p_{90,ref}$	$\overline{d}$	R_m	DE	$\Delta\lambda$	λ_2
$\Delta p_{50}/\Delta p_{50,ref}$	1.00 (1.00)	0.97 (0.97)	−0.98 (−0.96)	−0.98 (−0.96)	0.98 (0.96)	0.58 (0.52)	−0.97 (−0.97)
$\Delta p_{90}/\Delta p_{90,ref}$		1.00 (1.00)	−0.99 (−0.98)	−0.99 (−0.98)	0.99 (0.98)	0.57 (0.53)	−0.97 (−0.97)
$\overline{d}$			1.00 (1.00)	1.00 (1.00)	−1.00 (−1.00)	−0.58 (−0.56)	0.98 (0.98)
R_m				1.00 (1.00)	−1.00 (−1.00)	−0.58 (−0.56)	0.98 (0.98)
DE					1.00 (1.00)	0.58 (0.56)	−0.98 (−0.98)
$\Delta\lambda$						1.00 (1.00)	−0.57 (−0.54)
λ_2							1.00 (1.00)

4. Conclusions

The aim of this paper is to evaluate the effectiveness of some connectivity indicators in representing the alteration of the transient response of a system in the face of a change in its topological structure. To this end, five CMs drawn from graph theory (i.e., the average degree $\overline{d}$, the meshedness coefficient R_m, the number of single-degree nodes DE, the spectral gap $\Delta\lambda$, and the algebraic connectivity λ_2) have been considered. They are compared in terms of the ability to represent the dynamic behavior of two networks subjected to different transient scenarios, when their topological structure is modified by closing an increasing number of IVs. The main results are:

- topology modifications are confirmed to have an impact on the transient response of WDNs. In particular, as the number of branches increases and the number of interconnections and loops decreases, the pressure stress state of the network is emphasized;
- overall, the CMs show a correlation with the average and extreme transient response of a network. Precisely, $\overline{d}$, R_m, DE, and λ_2 are the metrics that most effectively reflect the dynamic behavior of the system, whereas $\Delta\lambda$ is not representative showing a scattered distribution;
- among the CMs that show a good performance in representing the dynamic behavior of a network (i.e., $\overline{d}$, R_m, DE, and λ_2), the three combinatoric-based metrics (i.e., $\overline{d}$, R_m, and DE) show a very strong correlation with the transient response of a network and, given their almost perfect correlation, considering one or the other of these three metrics is equivalent. The correlation coefficient of the algebraic connectivity λ_2 is slightly lower than the other metrics. In fact, the metrics that are more directly related to the number of nodes, links, loops and dead ends seem to better reflect the transient response of a WDN. This result confirms the significant impact that looped and tree-like structures have in the development of the dynamic behavior of a network. On the one hand, loops facilitate the fragmentation and the dampening of pressure waves whereas, a high number of dead ends emphasizes pressure waves and the global transient response of the system.

This paper shows that the use of CMs can be effectively extended from a steady-state framework to a dynamic one and their ability to represent the dynamic behavior of a WDN as its configuration changes could be exploited during network modification phases. Thus, the metrics could be effectively used for a preliminary evaluation of the impact of the sectorization of a system (e.g., in the case of DMAs creation or for the purpose of ensuring water quality) on the variation in the pressure stress to which it will be subjected once the modification is applied. In greater detail, these metrics clearly cannot provide a comprehensive characterization of the transient response of a WDN, as they are not able to provide all the information that could be obtained from a transient simulation taking into account factors, such as diameters and materials of pipes, or dominant frequencies. Despite this, graph theory metrics may serve to complement traditional physics-based computer models of WDNs by providing inexpensive proxies on system-level performance. From an operational standpoint, these metrics can help avoiding a significant number of simulations in unsteady-state conditions to be executed. In fact, the transient response of a network with a given connectivity, and therefore a related metric, can be easily approximated after the classification of a very small number of exact solutions, which may be evaluated for "extreme" network configurations, that is, highly looped or highly branched layouts.

The metrics considered in this paper represent an initial subset from a vast collection of graph theory properties already known in the literature. In this regard, further studies are ongoing to test the effectiveness of other known metrics and new ones that can also take into account pipe features affecting the development of pressure waves, such as pipe diameter and material. Moreover, additional research is needed to explore other complex real cases of WDNs and alternative transient scenarios with different forcing factors.

Data Availability Statement

Data are available at the following link: https://doi.org/10.5281/zenodo.8172321.

References

Abraham, E., Blokker, E. J. M., & Stoianov, I. (2017). Decreasing the discoloration risk of drinking water distribution systems through optimized topological changes and optimal flow velocity control. *Journal of Water Resources Planning and Management – ASCE*, *144*(2), 04017093. https://doi.org/10.1061/(ASCE)WR.1943-5452.0000878

Alderson, D. L. (2008). Catching the network science bug: Insight and opportunity for the operations researcher. *Operational Research*, *56*(5), 1047–1065. https://doi.org/10.1287/opre.1080.0606

Alvisi, S. (2015). A new procedure for optimal design of district metered areas based on the multilevel balancing and refinement algorithm. *Water Resources Management*, *29*(12), 4397–4409. https://doi.org/10.1007/s11269-015-1066-z

Alvisi, S., & Franchini, M. (2006). Near-optimal rehabilitation scheduling of water distribution systems based on a multi-objective genetic algorithm. *Civil Engineering and Environmental Systems*, *23*(3), 143–160. https://doi.org/10.1080/10286600600789300

Bergant, A., Simpson, A. R., & Vitkovsky, J. (2001). Developments in unsteady pipe flow friction modelling. *Journal of Hydraulic Research*, *39*(3), 249–257. https://doi.org/10.1080/00221680109499828

Boulos, P. F., Karney, B. W., Wood, D. J., & Lingireddy, S. (2005). Hydraulic transient guidelines for protecting water distribution systems. *Journal of the American Water Works Association*, *97*(5), 111–124. https://doi.org/10.1002/j.1551-8833.2005.tb10892.x

Brentan, B., Monteiro, L., Carneiro, J., & Covas, D. (2021). Improving water age in distribution systems by optimal valve operation. *Journal of Water Resources Planning and Management – ASCE*, *147*(8), 04021046. https://doi.org/10.1061/(ASCE)WR.1943-5452.0001412

Brunone, B., & Berni, A. (2010). Wall shear stress in transient turbulent pipe flow by local velocity measurement. *Journal of Hydraulic Engineering*, *136*(10), 716–726. https://doi.org/10.1061/(ASCE)HY.1943-7900.0000234

Brunone, B., & Golia, U. M. (2008). Discussion of "Systematic evaluation of one-dimensional unsteady friction models in simple pipelines" by Vitkovsky, J. P., Bergant, A., Simpson, A. R., Lambert, M. F. *Journal of Hydraulic Engineering*, *2*(282), 282–284. https://doi.org/10.1061/(ASCE)0733-9429(2008)134

Brunone, B., Golia, U. M., & Greco, M. (1995). Effects of two-dimensionality on pipe transients modelling. *Journal of Hydraulic Engineering*, *121*(12), 906–912. https://doi.org/10.1061/(ASCE)0733-9429(1995)121:12(906)

Chaudhry, H. M. (2014). *Applied hydraulic transients* (3rd ed.). Van Nostrand Reinhold.

Chondronasios, A., Gonelas, K., Kanakoudis, V., Patelis, M., & Korkana, P. (2017). Optimizing DMAs' formation in a water pipe network: The water aging and the operating pressure factors. *Journal of Hydroinformatics*, *19*(6), 890–899. https://doi.org/10.2166/hydro.2017.156

Diestel, R. (2005). *Graph theory* (3rd ed.). Springer.

Di Nardo, A., & Di Natale, M. (2011). A heuristic design support methodology based on graph theory for district metering of water supply networks. *Engineering Optimization*, *43*(2), 193–211. https://doi.org/10.1080/03052151003789858

Ebacher, G., Besner, M.-C., Lavoie, J., Jung, B. S., Karney, B. W., & Prévost, M. (2011). Transient modeling of a full-scale distribution system: Comparison with field data. *Journal of Water Resources Planning and Management*, *137*(2), 173–182. https://doi.org/10.1061/(ASCE)WR.1943-5452.0000109

Ellis, J. (2008). *Pressure transients in water engineering: A guide to analysis and interpretation of behaviour*. ICE Publishing.

Estrada, E. (2006). The interplay of expansibility and degree distribution. *The European Physical Journal B*, *52*(4), 563–574. https://doi.org/10.1140/epjb/e2006-00330-7

Farmani, R., Walters, G. A., & Savic, D. A. (2005). Trade-off between total cost and reliability for anytown water distribution network. *Journal of Water Resources Planning and Management – ASCE*, *131*(3), 161–171. https://doi.org/10.1061/(ASCE)0733-9496(2005)131:3(161)

Fiedler, M. (1973). Algebraic connectivity of graphs. *Czechoslovak Mathematical Journal*, *23*(98), 298–305. https://doi.org/10.21136/CMJ.1973.101168

Furnass, W. R., Mounce, S. R., & Boxall, J. B. (2013). Linking distribution system water quality issues to possible causes via hydraulic pathways. *Environmental Modelling & Software*, *40*, 78–87. https://doi.org/10.1016/j.envsoft.2012.07.012

Ghidaoui, M. S., Zhao, M., McInnis, D. A., & Axworthy, D. H. (2005). A review of water hammer theory and practice. *Applied Mechanics Reviews*, *58*(1), 49–76. https://doi.org/10.1115/1.1828050

Giudicianni, C., Di Nardo, A., Di Natale, M., Greco, R., Santonastaso, G. F., & Scala, A. (2018). Topological taxonomy of water distribution networks. *Water*, *10*(4), 444. https://doi.org/10.3390/w10040444

Giustolisi, O., & Ridolfi, L. (2014a). A new modularity-based approach to segmentation of water distribution networks. *Journal of Hydraulic Engineering*, *140*(10), 04014049. https://doi.org/10.1061/(ASCE)HY.1943-7900.0000916

Giustolisi, O., & Ridolfi, L. (2014b). A novel infrastructure modularity index for the segmentation of water distribution networks. *Water Resources Research*, *50*(10), 7648–7661. https://doi.org/10.1002/2014WR016067

Grayman, W. M., Murray, R., & Savic, D. A. (2009). Effects of redesign of water systems for security and water quality factors. In *Proceedings of the World Environmental and Water Resources Congress 2009*.

Hajebi, S., Roshani, E., Cardozo, N., Barrett, S., Clarke, A., & Clarke, S. (2016). Water distribution network sectorisation using graph theory and many-objective optimisation. *Journal of Hydroinformatics*, *18*(1), 77–95. https://doi.org/10.2166/hydro.2015.144

Huang, Y., Zheng, F., Kapelan, Z., Savic, D., Duan, H.-F., & Zhang, Q. (2020). Efficient leak localization in water distribution systems using multistage optimal valve operations and smart demand metering. *Water Resources Research*, *56*(10), e2020WR028285. https://doi.org/10.1029/2020WR028285

Karney, B. W., & McInnis, D. (1990). Transient analysis of water distribution systems. *Journal of the American Water Works Association*, *82*(7), 62–70. https://doi.org/10.1002/j.1551-8833.1990.tb06992.x

Mala-Jetmarova, H., Sultanova, N., & Savic, D. A. (2018). Lost in optimisation of water distribution systems? A literature review of system design. *Water*, *10*(3), 307. https://doi.org/10.3390/w10030307

Marquez Calvo, O. O., Quintiliani, C., Alfonso, L., Di Cristo, C., Leopardi, A., Solomatine, D., & de Marinis, G. (2018). Robust optimization of valve management to improve water quality in WDNs under demand uncertainty. *Urban Water Journal*, *15*(10), 943–952. https://doi.org/10.1080/1573062X.2019.1595673

Marsili, V., Meniconi, S., Alvisi, S., Brunone, B., & Franchini, M. (2021). Experimental analysis of the water consumption effect on the dynamic behaviour of a real pipe network. *Journal of Hydraulic Research*, *59*(3), 477–487. https://doi.org/10.1080/00221686.2020.1780506

Marsili, V., Meniconi, S., Alvisi, S., Brunone, B., & Franchini, M. (2022). Stochastic approach for the analysis of demand induced transients in real water distribution systems. *Journal of Water Resources Planning and Management – ASCE*, *148*(1), 04021093. https://doi.org/10.1061/(ASCE)WR.1943-5452.0001498

Meniconi, S., Brunone, B., & Frisinghelli, M. (2018). On the role of minor branches, energy dissipation, and small defects in the transient response of transmission mains. *Water*, *10*(2), 187. https://doi.org/10.3390/w10020187

Meniconi, S., Cifrodelli, M., Capponi, C., Duan, H.-F., & Brunone, B. (2021). Transient response analysis of branched pipe systems toward a reliable skeletonization. *Journal of Water Resources Planning and Management*, *147*(2), 04020109. https://doi.org/10.1061/(ASCE)WR.1943-5452.0001319

Meniconi, S., Maietta, F., Alvisi, S., Capponi, C., Marsili, V., Franchini, M., & Brunone, B. (2022a). Consumption change-induced transients in a water distribution network: Laboratory tests in a looped system. *Water Resources Research*, *58*(10), e2021WR031343. https://doi.org/10.1029/2021WR031343

Meniconi, S., Maietta, F., Alvisi, S., Capponi, C., Marsili, V., Franchini, M., & Brunone, B. (2022b). A quick survey of the most vulnerable areas of a water distribution network due to transients generated in a service line: A Lagrangian model based on laboratory tests. *Water*, *14*(17), 2741. https://doi.org/10.3390/w14172741

Misiunas, D. (2005). *Failure monitoring and asset condition assessment in water supply systems* (PhD Thesis). Lund University.

Newman, M. (2010). *Networks: An introduction* (1st ed.). Oxford University Press.

Perelman, L., Housh, M., & Ostfeld, A. (2013). Robust optimization for water distribution systems least cost design. *Water Resources Research*, *49*(10), 6795–6809. https://doi.org/10.1002/wrcr.20539

Pezzinga, G. (2000). Evaluation of unsteady flow resistances by Quasi-2D or 1D models. *Journal of Hydraulic Engineering*, *126*(10), 778–785. https://doi.org/10.1061/(ASCE)0733-9429(2000)126:10(778)

Pothof, I., & Karney, B. (2012). Guidelines for transient analysis in water transmission and distribution systems. In A. Ostfeld (Ed.), *Water supply system analysis: Selected topics*. InTech. https://doi.org/10.5772/53944

Prasad, T. D., & Park, N. S. (2004). Multiobjective genetic algorithms for design of water distribution networks. *Journal of Water Resources Planning and Management – ASCE*, *130*(1), 73–82. https://doi.org/10.1061/(ASCE)0733-9496(2004)130:1(73)

Quintiliani, C. (2017). *Water quality enhancement in WDNs through optimal valves setting* (PhD Thesis). University of Cassino and Southern Lazio.

Quintiliani, C., Marquez-Calvo, O., Alfonso, L., Di Cristo, C., Leopardi, A., Solomatine, D. P., & de Marinis, G. (2019). Multiobjective valve management optimization formulations for water quality enhancement in water distribution networks. *Journal of Water Resources Planning and Management – ASCE*, *145*(12), 04019061. https://doi.org/10.1061/(ASCE)WR.1943-5452.0001133

Rezaei, H., Ryan, B., & Stoianov, I. (2015). Pipe failure analysis and impact of dynamic hydraulic conditions in water supply networks. *Procedia Engineering*, *119*, 253–262. https://doi.org/10.1016/j.proeng.2015.08.883

Sirsant, S., & Reddy, M. J. (2020). Assessing the performance of surrogate measures for water distribution network reliability. *Journal of Water Resources Planning and Management – ASCE*, *146*(7), 04020048. https://doi.org/10.1061/(ASCE)WR.1943-5452.0001244

Sitzenfrei, R. (2021). Using complex network analysis for water quality assessment in large water distribution systems. *Water Resources*, *201*(1), 117359. https://doi.org/10.1016/j.watres.2021.117359

Starczewska, D., Collins, R., & Boxall, J. (2014). Transient behaviour in complex distribution network: A case study. *Procedia Engineering*, *70*, 1582–1591. https://doi.org/10.1016/j.proeng.2014.02.175

Strogatz, S. (2001). Exploring complex networks. *Nature*, *410*(6825), 268–276. https://doi.org/10.1038/35065725

Sundstrom, L. R. J., & Cervantes, M. J. (2017). Transient wall shear stress measurements and estimates at high Reynolds numbers. *Flow Measurement and Instrumentation*, *58*, 112–119. https://doi.org/10.1016/j.flowmeasinst.2017.10.003

Swaffield, J., & Boldy, A. (1993). *Pressure surges in pipe and duct systems*. Avebury Technical, Gower Press.

Todini, E. (2000). Looped water distribution networks design using a resilience index based heuristic approach. *Urban Water Journal*, *2*, 115–122. https://doi.org/10.1016/S1462-0758(00)00049-2

Todini, E., & Pilati, S. (1988). A gradient algorithm for the analysis of pipe networks. In B. Coulbeck & C.-H. Orr (Eds.), *Proc., computer application for water supply (Vol. 1–System analysis and simulation)* (Vol. 1–20). Wiley.

Torres, J. M., Duenas-Osorio, L., Li, Q., & Yazdani, A. (2016). Exploring topological effects on water distribution system performance using graph theory and statistical models. *Journal of Water Resources Planning and Management – ASCE*, *143*(1), 04016068. https://doi.org/10.1061/(ASCE)WR.1943-5452.0000709

Tzatchkov, V., Alcocer-Yamanaka, V., & Bourguett Ortíz, V. (2006). Graph theory based algorithms for water distribution network sectorization projects. In *Proceedings of the Water Distribution Systems Analysis Symposium 2006*. https://doi.org/10.1061/40941(247)172

Vardy, A. E., & Brown, J. M. B. (1996). On turbulent, unsteady, smooth pipe friction. In *7th Internationsl Conference on Pressure Surges and Fluid Transients in Pipelines and Open Channels* (Vol. 289–311). BHR Group.

Vreeburg, J. H. G., & Boxall, J. B. (2007). Discolouration in potable water distribution systems: A review. *Water Research*, *41*(3), 519–529. https://doi.org/10.1016/j.watres.2006.09.028

Wylie, E. B., & Streeter, V. L. (1993). *Fluid transients in systems*. Prentice-Hall Inc.

Yazdani, A., & Jeffrey, P. (2010). A complex network approach to robustness and vulnerability of spatially organized water distribution networks. https://doi.org/10.48550/arXiv.1008.1770

Yazdani, A., & Jeffrey, P. (2012). Applying network theory to quantify the redundancy and structural robustness of water distribution systems. *Journal of Water Resources Planning and Management – ASCE*, *138*(2), 153–161. https://doi.org/10.1061/(ASCE)WR.1943-5452.0000159

Zhang, Q., Wu, Z., Zhao, M., Qi, J., Huang, Y., & Zhao, H. (2017). Automatic partitioning of water distribution networks using multiscale community detection and multiobjective optimization. *Journal of Water Resources Planning and Management – ASCE*, *143*(9), 1–14. https://doi.org/10.1061/(ASCE)WR.1943-5452.0000819